Reference: *Biol. Bull.* **232:** 198–211. (June 2017)

Crossing the Divide: Admixture Across the Antarctic Polar Front Revealed by the Brittle Star *Astrotoma agassizii*

MATTHEW P. GALASKA[1,*], CHESTER J. SANDS[2], SCOTT R. SANTOS[1], ANDREW R. MAHON[3], AND KENNETH M. HALANYCH[1,*]

[1]*Molette Biology Laboratory for Environmental and Climate Change Studies, Department of Biological Sciences, Auburn University, 101 Rouse Life Sciences Building, Auburn, Alabama 36849;* [2]*British Antarctic Survey, Natural Environment Research Council, Cambridge CB3 0ET, United Kingdom; and* [3]*Department of Biology, Central Michigan University, Mount Pleasant, Michigan 48859*

Abstract. The Antarctic Polar Front (APF) is one of the most well-defined and persistent oceanographic features on the planet and serves as a barrier to dispersal between the Southern Ocean and lower latitudes. High levels of endemism in the Southern Ocean have been attributed to this barrier, whereas the accompanying Antarctic Circumpolar Current (ACC) likely promotes west-to-east dispersal. Previous phylogeographic work on the brittle star *Astrotoma agassizii* Lyman, 1875 based on mitochondrial genes suggested isolation across the APF, even though populations in both South American waters and the Southern Ocean are morphologically indistinguishable. Here, we revisit this finding using a high-resolution 2b-RAD (restriction-site-associated DNA) single-nucleotide polymorphism (SNP)-based approach, in addition to enlarged mitochondrial DNA data sets (*16S rDNA*, *COI*, and *COII*), for comparison to previous work. In total, 955 biallelic SNP loci confirmed the existence of strongly divergent populations on either side of the Drake Passage. Interestingly, genetic admixture was detected between South America and the Southern Ocean in five individuals on both sides of the APF, revealing evidence of recent or ongoing genetic contact. We also identified two differentiated populations on the Patagonian Shelf with six admixed individuals from these two populations. These findings suggest that the APF is a strong but imperfect barrier. Fluctuations in location and strength of the APF and ACC due to climate shifts may have profound consequences for levels of admixture or endemism in this region of the world.

Received 28 March 2017; Accepted 5 June 2017; Published online 1 September 2017.

* To whom correspondence should be addressed. E-mail: mattgalaska@gmail.com; ken@auburn.edu.

Abbreviations: ACC, Antarctic Circumpolar Current; APF, Antarctic Polar Front; BIC, Bayesian information criterion; RAD, restriction-site-associated DNA; SNP, single-nucleotide polymorphism.

Introduction

Although marine systems are often thought of as "open" to dispersal, strong oceanic barriers can exist, isolating populations over time and potentially leading to speciation (Clarke *et al.*, 2005; Thornhill *et al.*, 2008; Figuerola *et al.*, 2017). One of the strongest open ocean barriers in the world is the Antarctic Polar Front (APF), which isolates the Southern Ocean from warmer waters at lower latitudes and thus contributes to the high endemism found in the Southern Ocean (Thornhill *et al.*, 2008; Kaiser *et al.*, 2013). However, the APF co-occurs with the Antarctic Circumpolar Current (ACC), which functions as an oceanographic dispersal mechanism for many species in and around the Southern Ocean (Bathmann *et al.*, 1997; Smetacek *et al.*, 1997). Megafauna such as whales, fur seals, and marine birds freely move across the APF (Rasmussen *et al.*, 2007); but, in contrast, endemism is particularly high among several marine invertebrate groups inhabiting continental shelves on either side of the APF despite having long life-stages capable of dispersal (Ekman, 1953; Hempel, 1985; Arntz *et al.* 1997; Thatje, 2012). For example, molecular studies analyzing genetic connectivity across the APF have revealed distinct genetic breaks on either side

of the APF in nemertean worms (Thornhill *et al.*, 2008), octocorals (Dueñas *et al.*, 2016), and notothenioid fish (Bargelloni *et al.*, 2000). Although one study suggested that migration occurs across the APF in molluscs on the basis of taxonomy (Jörger *et al.*, 2014), supporting molecular data are absent, and these animals occurred at abyssal, not shelf, depths. Another group for which species are reported to occur on both sides of the ACC and APF is the Ophiuroidea, a dominant component of Southern Ocean benthic fauna (Stöhr *et al.*, 2012). For example, molecular work within the brittle star species *Ophiura lymani* identified successful radiations out of the Southern Ocean into South America, albeit only during the Pleistocene (Sands *et al.*, 2015). Presently, genetic connectivity has not been recognized across the APF among extant ophiuroids.

In contrast to the APF, the ACC is often considered to be a large-scale dispersal vector (Nikula *et al.*, 2010), moving clockwise around Antarctica and coming into contact with the southernmost region of South America. Pelagic larvae, such as lecithotrophic larvae produced by the brittle star *Astrotoma agassizii* Lyman, 1875, have been recovered from the Ross Sea with mitochondrial haplotypes matching those from the Antarctic Peninsula, presumably *via* dispersal by the ACC (Heimeier *et al.*, 2010). Additionally, the isopod species *Septemserolis septemcarinata*, which has no pelagic stages, can apparently disperse over a distance of 2000 km, likely through rafting on kelp mediated by the ACC (Leese *et al.*, 2010). Thus, if a species' life history incorporates a planktonic dispersal phase, migration to the Patagonian Shelf of South America, some ~700 km from the Antarctic shelf, is possible given the Coriolis effect and Eckman transport (Price *et al.*, 1988). However, such dispersal events across the APF would require that a species withstand substantial temperature and salinity changes. Previous trans-Drake Passage work on *A. agassizii* using mitochondrial DNA (mtDNA) identified a single clade on the shelf regions of the Southern Ocean and two clades on the South American shelf, with no evidence for genetic connectivity across the APF (Hunter and Halanych, 2008). However, geographic sampling in the Southern Ocean has previously been limited primarily to the Antarctic Peninsula, and genetic analyses relied solely on mtDNA, which is uniparentally inherited and not suitable for exploring potential admixture. Morphologically designated as a single species on either side of the Drake Passage, *A. agassizii* is considered a brooder in its geographic ranges of South America but has recently been revealed to possess planktonic lecithotrophic larvae in the Southern Ocean (Heimeier *et al.*, 2010). Whether these reproductive strategies are unique to either region is unknown, but this difference could imply that *A. agassizii* is composed of different species.

Here, we address the question of genetic connectivity in the brittle star *A. agassizii* (Fig. 1), which has a broad geographic distribution, by examining populations from both the Western Antarctic and the South American continental shelves. Specifically, we sampled a broader geographic range as well as a greater number of individuals than Hunter and Halanych (2008), using both mtDNA and higher-resolution genomic single-nucleotide polymorphism (SNP) markers with the 2b-RAD approach (Wang *et al.*, 2012), a restriction-site-associated DNA (RAD) genotyping method. A larger geographic range was included in this study for the Southern Ocean to facilitate investigation of spatial genetic structure within *A. agassizii*'s Southern Ocean circumpolar distribution. Similar 2b-RAD work on the circumpolar ophiuroid *Ophionotus victoriae* revealed four distinct populations that were geographically structured and may represent multiple species (Galaska *et al.*, 2017b). This was contrary to the prediction of an intermixed range due to the dispersal capabilities of *O. victoriae*'s feeding planktotrophic larvae. In this study, two hypotheses were tested: (1) Southern Ocean and South American lineages of *A. agassizii* are genetically isolated, representing distinct ecological and evolutionary units, and (2) significant genetic structure by geography would be recovered in the Southern Ocean, analogous to what was recently identified in *O. victoriae*.

Materials and Methods

Taxon sampling

Individuals of *Astrotoma agassizii* were collected during four National Science Foundation-sponsored research expeditions (*i.e.*, RVIB *Nathaniel B. Palmer* 12-10, RV *Laurence M. Gould* 04-14, 06-05, and 13-12), the *Polarstern* expedition PS77, and four British Antarctic Survey-sponsored expeditions (*i.e.*, JR144, JR179, JR230, and JR275). In total, the data set included 231 individuals collected from the Ross Sea to the Weddell Sea in the Southern Ocean and the Patagonian Shelf off the southeastern coast of South America (Fig. 2a; Table S1, available online).

Sample preparation and sequencing

Genomic DNA was extracted using a DNeasy Blood and Tissue Kit (Qiagen, Hilden, Germany) following the manufacturer's protocol, and fragments from three mtDNA genes (*i.e.*, cytochrome *c* oxidase subunits I [*COI*] and II [*COII*] and the large ribosomal subunit *16S-rDNA*) were amplified *via* polymerase chain reaction. Samples from 45 individuals that were provided by and analyzed at the British Antarctic Survey were amplified for an ~660-bp fragment of *COI* with the primers LCO1490 (5′-GGTCAACAAATCATAAAGATATTGG-3′) and HCO2198 (5′-TAAACTTCAGGGTGACCAAAAAATCA-3′) (Folmer *et al.*, 1994) under the following thermocycling conditions: initial denaturation at 94 °C for 3 min, 40 cycles of denaturation at 94 °C for 30 s, annealing at 51 °C for 1 min, extension at 72 °C for 1 min; and final extension at 72 °C for 2 min. Samples obtained by the Halanych Laboratory at Auburn

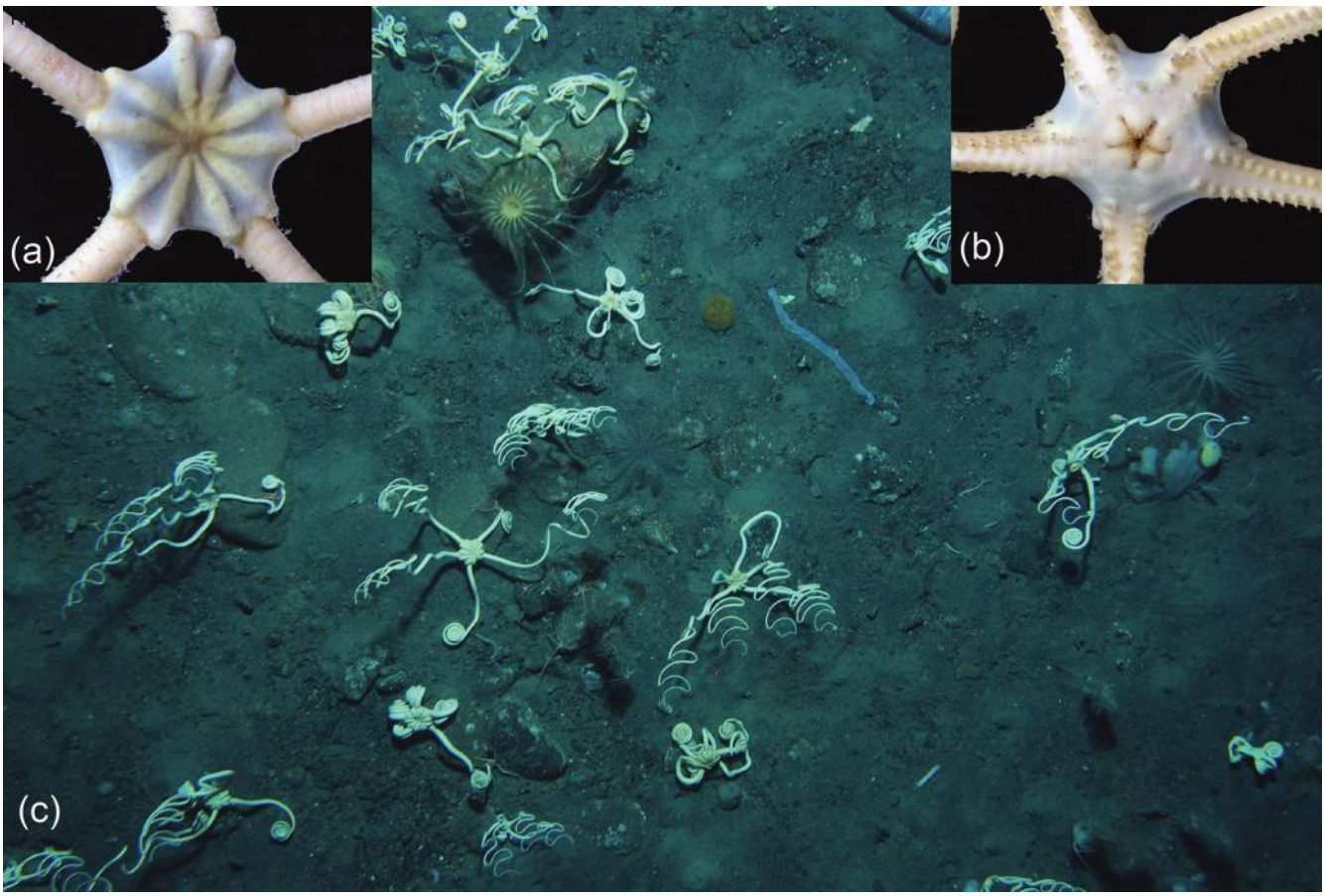

Figure 1. (a) Aboral view of *Astrotoma agassizii*. (b) Oral view of *A. agassizii*. (c) Yo-yo camera photo of the Southern Ocean benthic ecosystem where *A. agassizii* is the dominant species. Image was taken at a depth of 390 m in the Ross Sea at 74°10.9186 S, 166°39.6616 E. Photographs (a) and (b) are kindly provided by Dr. Christoph Held, © C. Held, AWI.

University from an additional 186 individuals were amplified and sequenced for fragments of the *COII* and *16S-rDNA* mtDNA genes to allow comparison to the work done by Hunter and Halanych (2008). The *COII* primer set CO2_23AF (5′-MCARCTWGGWTTWCAAGA-3′) and CO2_577R (5′-TCSGARCATTGSCCATARAA-3′) (Hunter and Halanych, 2008) was utilized to amplify an ~550-bp fragment from the same 186 individuals for which *16S-rDNA* was amplified (see below; Fig. 2; Table S1, available online). Thermocycling conditions utilized for *COII* were as follows: initial denaturation at 94 °C for 3 min; 35 cycles of denaturation at 94 °C for 30 s, annealing at 50 °C for 30 s, and extension at 72 °C for 30 s; and final extension at 72 °C for 3 min. An ~500-bp fragment of *16S-rDNA* was amplified using the primers 16SarL (5′-CGCCTGTTTATCAAAAACAT-3′) and 16SbrH (5′-CCGGTCTGAACTCAGATCACGT-3′) (Palumbi, 2007) under the following thermocycling conditions: initial denaturation at 94 °C for 3 min, 35 cycles of denaturation at 94 °C for 30 s, annealing at 46 °C for 30 s, extension at 72 °C for 30 s, and final extension at 72 °C for 3 min. Amplicons from *COII* and *16S-rDNA* were sent to Genewiz (South Plainfield, NJ) for bidirectional Sanger sequencing.

Population genetic analyses

Assembly and editing of bidirectional Sanger sequences were done with Sequencher software (ver. 5.4; Gene Codes, Ann Arbor, MI), and MEGA software (ver. 6; Tamura *et al.*, 2013) was used to perform alignments *via* MUSCLE software (Edgar, 2004) for each mtDNA gene. Network analyses using the TCS program were done with POPART software (ver. 1.7; Clement *et al.*, 2000; Leigh and Bryant, 2015) to visualize relationships between mtDNA haplotypes of *A. agassizii* recovered from *COI*, *COII*, and *16S-rDNA* separately, along with a concatenation of *16S-rDNA* and *COII* for all individuals that were sequenced for both (Fig. 3). DnaSP software (ver. 5.10.01; Librado and Rozas, 2009) was used to perform tests of neutrality, including Tajima's *D* (Ta-

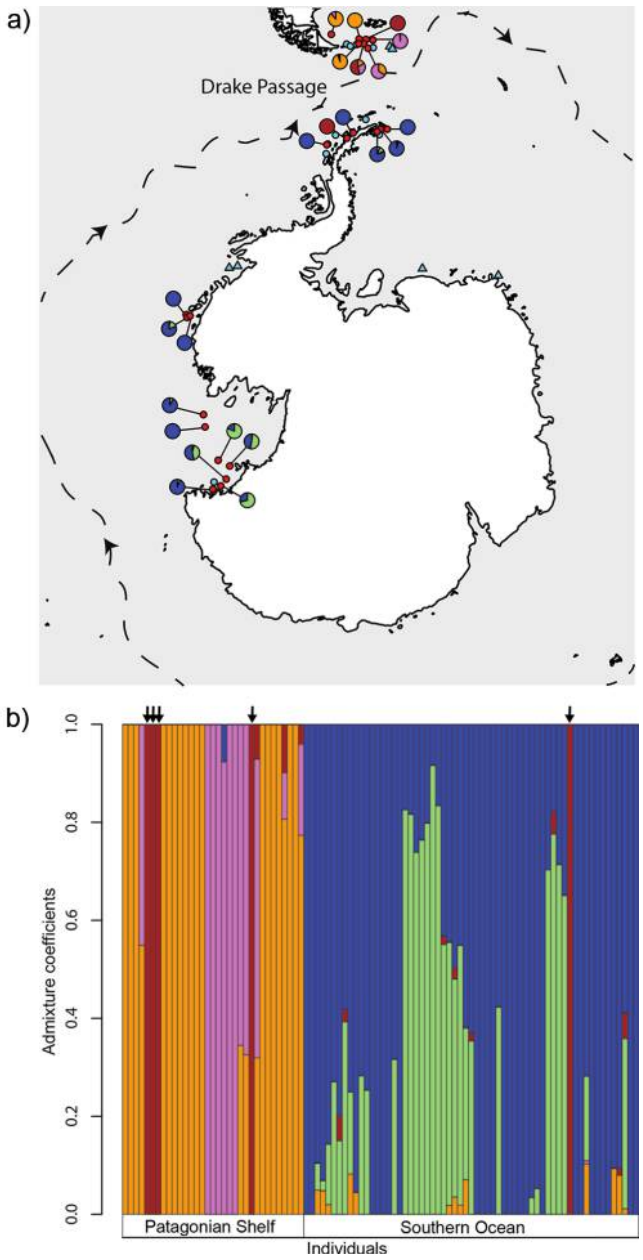

Figure 2. (a) Sampling locations of *Astrotoma agassizii* and admixture results from single-nucleotide polymorphism (SNP) analyses. Small red circles represent sampling localities for individuals with both nuclear 2b-RAD (restriction-site-associated DNA) and mitochondrial *COII* and *16S-rDNA* data. Light blue circles represent localities with *COII* and *16S-rDNA* data, and light blue triangles represent localities with *COI* data. Because of the proximity of some localities, small red circles had priority, as they included the most data and may overlap with proximal light blue circles. Pie charts connected to each small red circle represent the level of admixture that was found in the sampling locality recovered from LEA analyses (Frichot and François, 2015). The burgundy color (shown in pie charts and bar charts) represents individuals that are admixed between genotypes common to South America and the Southern Ocean. The dashed line with arrowheads represents the approximate location and direction of the Antarctic Polar Front and the Antarctic Circumpolar Current. (b) LEA admixture coefficients per individual, represented in a bar graph. Admixture coefficients are represented on the *y*-axis, and individuals are represented by a single vertical bar. Arrows along the top of the bar graph denote admixed individuals between the two regions.

jima, 1989) and Fu and Li's F_s (Fu and Li, 1993), along with standard nucleotide indices from each of the three mtDNA fragments. Uncorrected pairwise distances (*p*-distances) among the *COI*, *COII*, and *16S-rDNA* fragments were generated separately in PAUP* software (ver. 4.0b10; Swofford, 2003).

RAD-based SNP data collection

From the 231 individuals included in this study, a subset of 94 individuals were haphazardly selected for whole-genome SNP-based analyses following Wang *et al.*'s (2012) 2b-RAD protocol. These 94 individuals represented localities from the entire geographic range where both *COII* and *16S-rDNA* were also sampled. The 2b-RAD protocol utilized RNAse-treated genomic DNA that was cut with the restriction enzyme AlfI, which leaves a 2-bp sticky end on both sides of the cleaved DNA. A one-sixteenth reduction scheme was employed through the addition of site-specific ligation adaptors (specifically, NG/NG) that paired with their complementary 2-bp sticky ends. Samples were then dual barcoded and sent for sequencing to the HudsonAlpha Institute for Biotechnology Genome Services Laboratory (Huntsville, AL) on an Illumina Hi-Seq 2500 system (Illumina, San Diego, CA) using v4 chemistry, generating 50-bp single-end reads.

Raw Illumina reads were demultiplexed by sample, quality filtered, and aligned against a custom-derived reference built *de novo* from our sequences, as outlined in Wang *et al.* (2012), using scripts from Meyer (2017) and Stacks (ver. 1.35) denovo_map.pl (Catchen *et al.*, 2011). The 2b-RAD data were first filtered to exclude loci with less than 25× coverage within samples. Homozygous SNP loci were then defined to have a maximum variance of 1%, whereas those considered heterozygous had a minimum variance of 25%. Any loci that did not meet these criteria were excluded from further analyses. Finally, only loci occurring in ≥75% of individuals within a sampling locality were retained.

Multiple analyses were conducted on the SNP data set to determine genetic diversity and structure within and between geographic populations and genetic lineages of *A. agassizii*. Initially, SNP data were analyzed using discriminant analysis of principal components (DAPC) from the adegenet package (ver. 1.4-2; Jombart, 2008; Jombart *et al.*, 2010; Jombart and Ahmed, 2011) in the R statistical environment (ver. 3.3.2; R Core Team, 2016). Specifically, adegenet initially conducts a series of principal component analyses (PCAs) on SNP data that is then retained to perform a discriminant analysis on all PCAs (DAPC). Performing multiple PCAs allows for identification of genetic clusters while avoiding assumptions of population genetic models (Jombart *et al.*, 2010). The retention of multiple PCAs can then be analyzed by DAPC for group variability while avoiding within-group variation (Jombart *et al.*, 2010). Optimal clusters (K), likely representing discrete populations, were identified through Bayesian information criterion likelihood values from retained principle com-

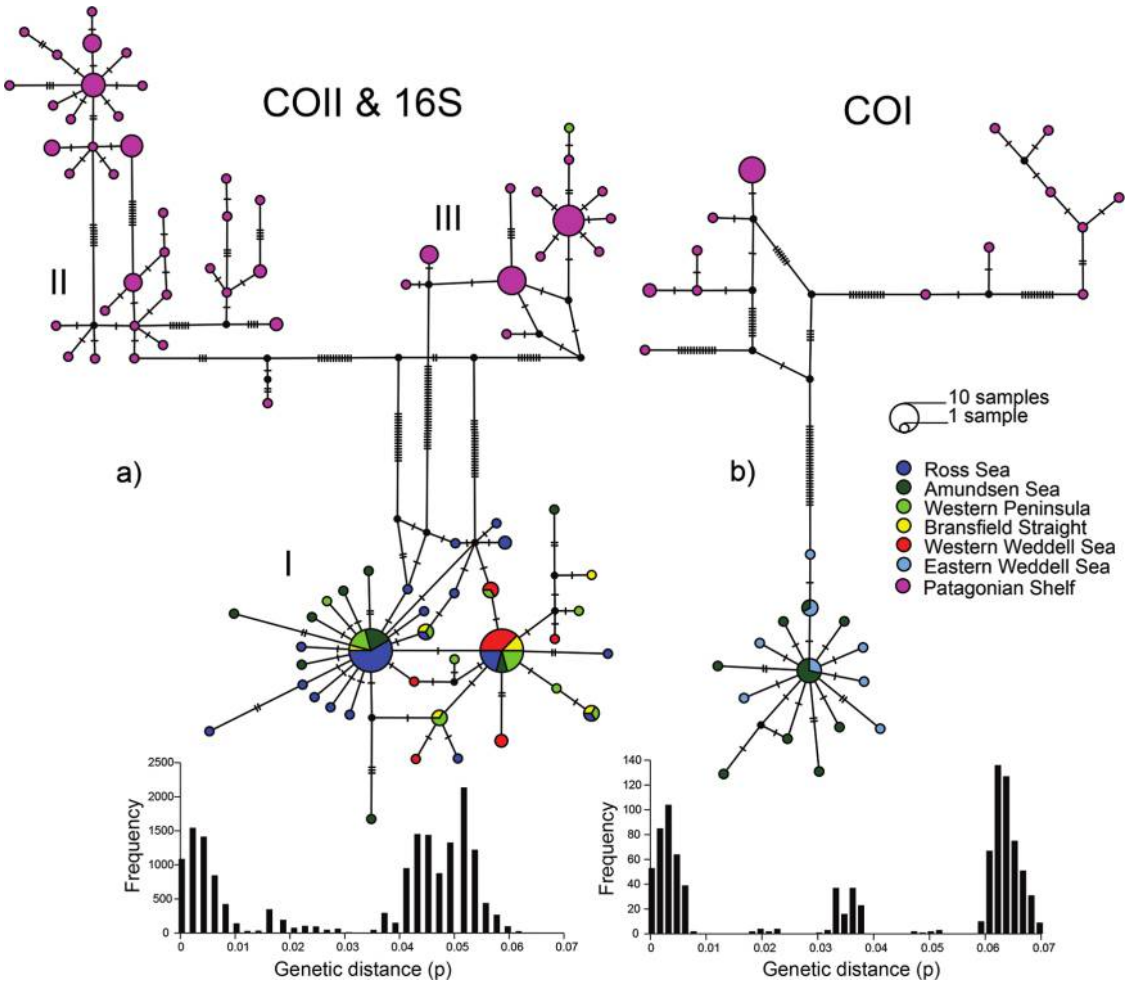

Figure 3. Haplotype network of *Astrotoma agassizii*. (a) Network based off *COII* and *16S-rDNA* data from 186 individuals along with uncorrected pairwise distances (*p*-distances) for *COII* located below the network. Clades I, II, and III in the *COII* and *16S-rDNA* haplotype network separate if a 95% connection limit is applied. (b) Network based off 45 individuals for which *COI* was amplified along with *p*-distances for *COI* located below the network. Filled black circles represent missing haplotypes.

ponents (Fig. A1). Visualization of DAPCs was performed with adegenet in R.

In addition, the LEA (landscape and ecological associations) package (ver. 1.0) in R was used to perform population structure inference and admixture coefficient analyses (Frichot and François, 2015). Estimation of K in LEA is performed using the cross-entropy criterion (Fig. A2), and least squares estimates were used to calculate ancestry proportions (Frichot *et al.*, 2014). Admixture was then visualized in two ways: (1) as bar charts, similar to those from STRUCTURE software (see below), and (2) as pie charts, with the inclusion of geographic coordinates to visualize admixture at each locality, which were overlain onto an orthographic projection map of Antarctica and the Patagonian Shelf with the R package ggplot2 (ver. 2.2.1; Wickham, 2009).

Further analyses of SNP data were performed using STRUCTURE (ver. 2.3.4; Pritchard *et al.*, 2000) under the following parameters: (1) five replicates at each potential K (1–18), (2) an admixture model with correlated allele frequencies, (3) a 100,000-generation burn-in period, and (4) 100,000 additional Markov chain Monte Carlo generations. These analyses were run on Southern Ocean and South American populations together as well as for each region separately. Files containing each simulation were then processed with STRUCTURE HARVESTER (ver. 0.6.94; Earl and VonHoldt, 2012) to objectively select a value for K on the basis of ΔK analyses. The selected K for each analysis was visualized using CLUMPP software (ver. 1.1.2; Jakobsson and Rosenberg, 2007) as well as DISTRUCT software (ver. 1.1; Rosenberg, 2004).

Last, summary statistics for SNP data along with analyses of genetic differentiation were performed in the R package HIERFSTAT (ver. 0.04-22; Goudet, 2005). Initially, SNP data were analyzed assuming a single population to recover summary statistics. However, once discrete populations were identified from the DAPC, LEA, and STRUCTURE analyses, additional summary statistics were performed on each. Pairwise F_{ST} differences were calculated using GenoDive software (ver. 2.0b27; Meirmans and Van Tienderen, 2004) to test for significance between the Southern Ocean and South American lineages.

Results

mtDNA

Sequence data for mtDNA *COII* and *16S-rDNA* were analyzed both separately and concatenated for 186 individuals (data set A) with an additional 45 individuals analyzed solely for *COI* (data set B), and all three mtDNA fragments revealed genetic structure between the Southern Ocean and South America. The TCS-based haplotype network of *Astrotoma agassizii* inferred from *COII* and *16S-rDNA* identified one clade in the Southern Ocean (clade I) and two distinct clades in South America (clades II and III) (Fig. 3a). Although the two South American clades are presented as a single network to show the relationship between them, they separate into distinct networks if a 95% connection limit is applied (data not shown). Notably, an individual with both *COII* and *16S-rDNA* haplotypes thought to be unique to South America was recovered on the Antarctic Peninsula in the Southern Ocean. Histograms of uncorrected *p*-distance values (Fig. 3) revealed two distinct modes in the *COII* and *16S-rDNA* concatenated data set, representing within-clade (0.2%–1.0%) and between-clade (3.8%–6.2%) genetic distances. Similar network results were recovered from 45 individuals analyzed for only *COI* (Fig. 3b), although inferences made from the *COI* data set are limited because there are fewer samples. Two similar modes for *COI* uncorrected *p*-distances were recovered for within (0.2%–0.8%) and between (5.8%–7.0%) clades.

Tests of neutrality were found to be not significant for either Tajima's *D* or Fu and Li's F_s for any of the three mtDNA fragments when data sets included all samples, which could be the result of differentiation between populations. Thus, additional tests of neutrality were performed individually on clades identified from network analyses (Fig. 3) for the *COII* fragment, since it consisted of the same number of individuals as *16S-rDNA* but possessed higher nucleotide diversity. In this case, Tajima's *D* and Fu and Li's F_s were found to be statistically significant ($P < 0.05$) and negative for clade I, with values of -2.217 and -3.89, respectively. Tests of neutrality in clade II were all found to be nonsignificant, while clade III was found to have a statistically significant and negative value for Fu and Li's F_s (-2.751; $P < 0.05$). Thus, these negatively significant tests of neutrality within clades I and III suggest either recent population expansions or purifying selection operating on *COII*, which are fairly typical results from mitochondrial data (Wares, 2010). Amplified fragments of *COI*, *COII*, and *16S-rDNA* recovered 76, 74, and 30 segregating sites, respectively, and summary nucleotide indices by fragment are presented in Table 1.

2b-RAD

Quality filtering of SNP loci yielded a data set of 955 polymorphic SNP loci among 94 individuals from the *COII* and *16S-rDNA* data sets, with 33 and 61 from the South America and Southern Ocean sampling localities, respectively (including the individual from the Southern Ocean that was recovered with a South American mtDNA haplotype). For the entire data set, the highest supported *K* for both DAPC and LEA was $K = 5$ (Figs. A1, A2), with two *K*s each in South America and the Southern Ocean and a fifth *K* composed of five individuals from the two geographic regions (*i.e.*, 4 from South America and 1 from the Southern Ocean; Figs. 2b, 4). Similar patterns were obtained when each region was analyzed individually (data not shown). As STRUCTURE has hierarchal model assumptions that are not always met (Jombart *et al.*, 2010; Kalinowski, 2011), the results, though similar, are presented in Figures A3–A5 for comparison. Although estimates for the number of discrete populations, as represented by *K*, were consistent between analyses, the true value likely resides somewhere within the range 2–5. Hereafter, the discussion of results assumes $K = 5$, given the above. Genetic distances between populations as defined by mitochondrial clade are presented in Table 2 and revealed significant ($P < 0.001$) differentiation between the three (*i.e.*, SOI, SAII, and SAIII). Summary estimates of genetic diversity recovered from the entire SNP data matrix are presented in Table 3. Fixed differences between clusters identi-

Table 1

Nucleotide indices from all three mtDNA fragments

	16S-rDNA	*COI*	*COII*
Nucleotide diversity (π)	0.018	0.038	0.032
No. of segregating sites	30	76	74
No. of parsimony-informative sites	22	60	53
Tajima's *D* statistic	1.154 ($P > 0.10$)	0.925 ($P > 0.10$)	0.102 ($P > 0.10$)
Fu and Li's F_s	-0.366 ($P > 0.10$)	0.294 ($P > 0.10$)	-1.475 ($P > 0.10$)
Hd	0.772 (SD, 0.001)	0.946 (SD, 0.000)	0.937 (SD, 0.009)

Note that neither Tajima's *D* nor Fu and Li's F_s tests of neutrality were found to be significant for any mitochondrial fragments. Hd, haplotype diversity.

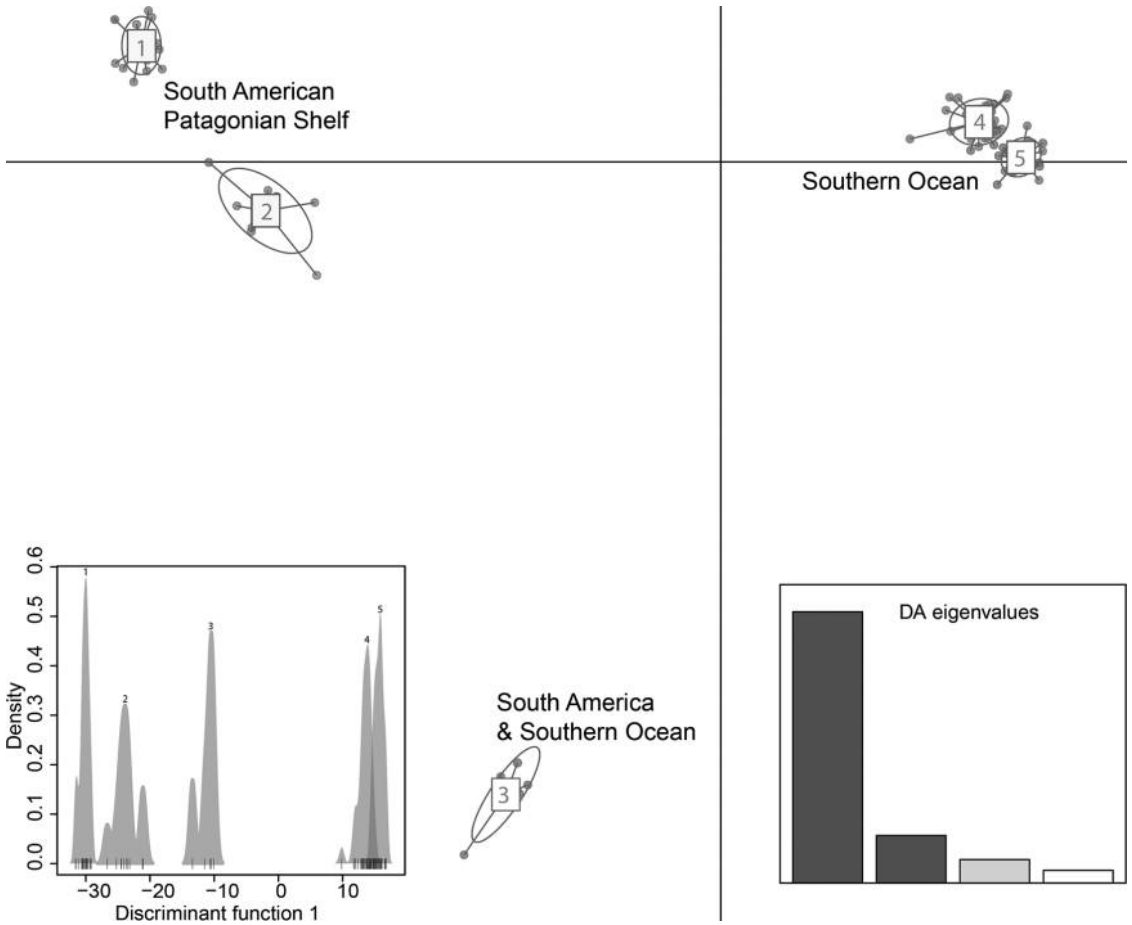

Figure 4. Discriminant analyses of principal components for *Astrotoma agassizii* in both the Southern Ocean and South America based on single-nucleotide polymorphism data. The numbers on each cluster are also presented on each peak in the histogram of density based on the discriminant function. DA, discriminant analysis.

fied by DAPC are presented in Table 4. Analyses of the Southern Ocean and South American data as a whole also yielded significant results ($F_{ST} = 0.721$, $P < 0.001$), supporting our first hypothesis that the two regions are genetically isolated. However, the second hypothesis of geographic structure in the Southern Ocean was found to be not significant ($F_{ST} = 0.002$, $P = 0.72$) from DAPC and LEA analyses.

Admixture

Notably, five individuals were identified apparently resulting from admixture, or genetic mixing, between populations in South America and the Southern Ocean, including one individual from the Southern Ocean possessing a South American mtDNA haplotype. These admixed individuals were recovered in the above analyses (in Fig. 2b, burgundy bars; in Fig. 4, cluster 3) and identified as such under all values of $K \geq 2$ (Figs. A3, A5, A6). Admixture was also recovered from six individuals between the two South American populations (Fig. 2b, bars with pink and yellow). These individuals were also distinguishable when SNP calls were manually scanned, because loci that were fixed in either South America or Southern Ocean populations were heterozygous in admixed individuals (note that admixed individuals may be F_2, F_3, or later generations, and thus not all admixed loci are heterozygous). Additionally, no unique alleles were detected in these apparently admixed individuals.

Discussion

Admixture across the APF

Using a suite of 955 polymorphic SNP loci for *Astrotoma agassizii*, we found evidence of admixture across the Drake Passage that separates the South American and Southern Ocean regions (Fig. 2b). Nonetheless, the South American and Southern Ocean lineages previously identified by Hunter and Halanych (2008) are confirmed to be strongly divergent populations ($F_{ST} = 0.721$, $P < 0.001$). Whereas analyses presented here and by others (Hunter and Halanych, 2008; Leese *et al.*, 2008; Thornhill *et al.*, 2008) do reveal significant genetic differentiation between populations in South America and the

Table 2

Pairwise F_{ST} *genetic distances for the single-nucleotide polymorphism data set between the three mtDNA clades (roman numerals are as in Fig. 3) recovered from both Hunter and Halanych (2008) and mtDNA analyses presented here*

	SOI	SAII	SAIII
SOI	. . .		
SAII	0.799	. . .	
SAIII	0.711	0.363	. . .

All F_{ST} values recovered have $P < 0.001$. SA, South America; SO, Southern Ocean.

Southern Ocean, SNP data allowed identification of admixed individuals implying recent, or even current, gene flow occurring bidirectionally across the strong barrier imposed by the APF. Moreover, we support earlier findings (*e.g.*, Hunter and Halanych, 2008) of two clades in South America with SNP-based analyses ($F_{ST} = 0.363$, $P < 0.001$), with admixture between them revealed in six individuals (Fig. 2b). For the Southern Ocean, SNP data also imply some geographic structure, particularly in the Ross Sea. Notably, the variable genetic structure of *A. agassizii* across the Southern Ocean contrasts with that of *Ophionotus victoriae*, which possesses population structure reflecting specific geographic regions (Galaska *et al.*, 2017b). In comparison, although both *A. agassizii* and *O. victoriae* in the Southern Ocean have been previously reported to have circumpolar distributions and employ broadcast spawning with planktonic larval life-history stages, *A. agassizii* appears to have higher dispersal capabilities relative to *O. victoriae*.

Asymmetric migration

With the unexpected findings of admixture across the APF, important questions arise, including just how permeable the APF is to dispersal of benthic invertebrates. Of course, the rate at which gene flow occurs is likely taxa dependent, and our limited sampling serves as just a coarse estimate at best. Even under these limitations, notable patterns are apparent. For instance, 12.1% of South American individuals sampled for 2b-RAD were apparently admixed between the two regions, compared with 1.6% from the Southern Ocean. That admixed individuals had a higher frequency in South America suggests that, in *A. agassizii*, migration is more probable from the Southern Ocean to South America. In recent evolutionary history, dispersal from the Southern Ocean to South America has also been identified in the ophiuroid species *Ophiura lymani* (Sands *et al.*, 2015). Alternatively, survivorship of admixed individuals could be more favorable in South America. Given that many benthic invertebrates in the Southern Ocean possess reproductive strategies involving a pelagic larval stage (Stanwell-Smith *et al.*, 1999) along with the dispersal potential of the ACC, the use of fine-scale population genetic techniques is likely to uncover a higher number of taxa having trans-APF connectivity.

Data presented here imply that *A. agassizii* individuals (most likely larvae) have an ability to migrate long distances (*i.e.*, >900 km) as well as overcome the 3–4 °C temperature cline at the APF between the Southern Ocean and South America. Genetic connectivity by teleplanic larvae is plausible through transport by mesoscale eddies generated by the ACC (Joyce *et al.*, 1981; Johnson and Bryden, 1989; Clarke *et al.*, 2005). Although such connectivity may occur in both northerly and southerly directions, given that the Antarctic Peninsula is experiencing unprecedentedly rapid warming due to climate change, higher-temperature waters have been suggested to mitigate migration of cold temperature–limited species (Aronson *et al.*, 2007, 2009; Clarke *et al.*, 2007). Additionally, warming temperatures along the Antarctic Peninsula could increase the survivability of individuals from northern latitudes on the Antarctic continental shelf (Meredith and King, 2005). Given this, one possible driver for the higher rate of admixture found in South America is that the temperature and salinity in more northerly latitudes may be

Table 3

Summary statistics for the 955 single-nucleotide polymorphism loci, inferred from the clusters identified by discriminant analyses of principal components as well as the complete data set

Region (cluster)	n	H_O	H_E	H_S	H_T	D_{ST}	H_{TP}	F_{ST}	F_{STP}	F_{IS}
SA (1)	19	0.097	0.093	0.0867	0.094	0.007	0.098	0.074	0.111	−0.130
SA (2)	10	0.106	0.085	0.095	0.096	0.001	0.095	0.006	0.013	−0.123
Admixed (3)	5	0.067	0.056	0.067	0.065	−0.002	0.063	−0.035	−0.048	−0.004
SO (4)	27	0.155	0.158	0.161	0.157	−0.003	0.157	−0.020	−0.024	0.068
SO (5)	33	0.158	0.159	0.160	0.164	0.004	0.167	0.025	0.038	0.026
SA and SO	94	0.136	0.373	0.122	0.372	0.250	0.438	0.671	0.721	0.027

Statistics are as follows: number of individuals (n), observed heterozygosity (H_O), expected heterozygosity (H_E), mean gene diversity within a population (H_S), overall gene diversity (H_T), gene diversity among samples (D_{ST}), corrected gene diversity (H_{TP}), global population differentiation (F_{ST}), corrected population differentiation (F_{STP}), and inbreeding coefficient (F_{IS}). Numbers in parentheses represent cluster numbers presented in Figure 4. SA, South America; SO, Southern Ocean.

Table 4

Number of fixed single-nucleotide polymorphism loci between the five clusters inferred from discriminant analyses of principal components

	SA (1)	SA (2)	SO (4)	SO (5)
SA (1)	. . .			
SA (2)	1	. . .		
SO (4)	287	292	. . .	
SO (5)	295	300	0	. . .
Heterozygous	233	217	452	425

Loci had to be 100% fixed for opposite alleles within the two compared populations to be counted. The final row is the number of loci coded for both alleles within a population. Numbers in parentheses represent cluster numbers presented in Figure 4. SA, South America; SO, Southern Ocean.

increasingly favorable to *A. agassizii*'s reproduction, as they have been implicated as important cues in other echinoderms (Lamare and Stewart, 1998). Migration of species or populations from South America could have played a crucial role in the Antarctic shelf undergoing recolonization after the postglacial maximum (Aronson *et al.*, 2007; Thatje, 2012).

Given that the Southern Ocean population of *A. agassizii* appears to be primarily reproducing *via* lecithotrophic larvae and that the South American population is described as brooding, recovering five individuals resulting from apparent admixture between them is surprising. Although we have conservatively considered the two regions to be distinctly diverged populations due to large genetic differentiation between the Southern Ocean and South America ($F_{ST} = 0.721$, $P < 0.001$), we recognize that *A. agassizii* may represent multiple species. This conclusion is supported by apparent reproductive differences and large genetic differences, with almost a third of the SNP loci fixed between regions (Table 4). However, morphological support for separate species is lacking.

Given that the Southern Ocean *A. agassizii* possess a pelagic larval stage, detection of more admixture on the Patagonian Shelf, although by limited sampling, would support the idea that migration from the Southern Ocean to South America is more common than the converse. However, explaining the introgression of the individual with the South American haplotype sampled from Antarctica is more difficult. For other animals, passive transport by rafting on substrate such as soft coral or macroalgae has been suggested (Leese *et al.*, 2010; Thatje, 2012) and documented (Helmuth *et al.*, 1994) in benthic invertebrates around the Southern Ocean. If South American *A. agassizii* do have a planktonic lecithotrophic larval stage, transport into the Southern Ocean *via* currents or mesoscale eddies may be possible. With the apparent higher rate of admixture found on the Patagonian Shelf of South America, this area and the western Chilean side of southern South America are areas of high interest for future research. If a first-generation migrant is going to be recovered from the Southern Ocean in South America, we hypothesize that the Chilean side of South America would be an ideal location to sample, as it is where the Humboldt Current breaks north from the ACC and comes into contact with the South American continent (White and Peterson, 1996). With the warming climate in the Southern Ocean, specifically around the Antarctic Peninsula (Meredith and King, 2005), the APF's ability to serve as an absolute barrier for many species could account for genetic isolation; but additional assessment of trans-APF species with high-resolution molecular techniques will likely yield more cases of connectivity.

Acknowledgments

We thank the National Science Foundation (NSF ANT-1043670 to ARM, NSF ANT-1043745 and OPP-0132032 to KMH) and the British Antarctic Survey for the funding to collect the specimens and perform the research. This research was made possible with assistance from the captains and crews of NBP12-10, LMG13-12, LMG04-14, LMG06-05, PS77, JR144, JR179, and JR230. We also thank Dr. Stephen Sefick for useful suggestions with ggplot2 in R. This is Molette Biology Laboratory contribution 65 and Auburn University Marine Biology Program contribution 159.

Data Accessibility

All sequences collected herein are reported under GenBank accession numbers KY986584–KY986640 (Fig. 2; Table S2, available online). Raw reads for 2b-RAD SNP data are deposited in the Sequence Read Archive (SAMN07237772–SAMN07237865). Data matrices and alignments are deposited in Dryad (see Galaska et al., 2017a).

Literature Cited

Arntz, W. E., J. Gutt, and M. Klages. 1997. Antarctic marine biodiversity: an overview. Pp. 3–14 in *Antarctic Communities: Species, Structure and Survival*, B. Battaglia, J. Valencia, and D. W. H. Walton, eds. Cambridge University Press, Cambridge.

Aronson, R. B., S. Thatje, A. Clarke, L. S. Peck, D. B. Blake, C. D. Wilga, and B. A. Seibel. 2007. Climate change and invasibility of the Antarctic benthos. *Annu. Rev. Ecol. Evol. Syst.* **38:** 129–154.

Aronson, R. B., R. M. Moody, L. C. Ivany, D. B. Blake, J. E. Werner, and A. Glass. 2009. Climate change and trophic response of the Antarctic bottom fauna. *PLoS One* **4:** e4385.

Bargelloni, L., S. Marcato, L. Zane, and T. Patarnello. 2000. Mitochondrial phylogeny of notothenioids: a molecular approach to Antarctic fish evolution and biogeography. *Syst. Biol.* **49:** 114–129.

Bathmann, U. V., R. Scharek, C. Klaas, C. D. Dubischarr, and V. Smetacek. 1997. Spring development of phytoplankton biomass and composition in major water masses of the Atlantic sector of the Southern Ocean. *Deep Sea Res. Part II Top. Stud. Oceanogr.* **44:** 51–67.

Catchen, J. M., A. Amores, P. Hohenlohe, W. Cresko, and J. H. Postlethwait. 2011. Stacks: building and genotyping loci *de novo* from short-read sequences. *G3 Genes Genomes Genet.* **1:** 171–182.

Clarke, A., D. K. A. Barnes, and D. A. Hodgson. 2005. How isolated is Antarctica? *Trends Ecol. Evol.* **20:** 1–3.

Clarke, A., N. M. Johnston, E. J. Murphy, and A. D. Rogers. 2007. Introduction. Antarctic ecology from genes to ecosystems: the impact of climate change and the importance of scale. *Philos. Trans. R. Soc. Lond. B Biol. Sci.* **362:** 5–9.

Clement, M., D. Posada, and K. A. Crandall. 2000. TCS: a computer program to estimate gene genealogies. *Mol. Ecol.* **9:** 1657–1659.

Dueñas, L. F., D. M. Tracey, A. J. Crawford, T. Wilke, P. Alderslade, and J. A. Sánchez. 2016. The Antarctic Circumpolar Current as a diversification trigger for deep-sea octocorals. *BMC Evol. Biol.* **16:** 2.

Earl, D. A., and B. M. VonHoldt. 2012. STRUCTURE HARVESTER: a website and program for visualizing STRUCTURE output and implementing the Evanno method. *Conserv. Genet. Resour.* **4:** 359–361.

Edgar, R. C. 2004. MUSCLE: multiple sequence alignment with high accuracy and high throughput. *Nucleic Acids Res.* **32:** 1792–1797.

Ekman, S. 1953. *Zoogeography of the Sea*. Sidgwick & Jackson, London.

Falush, D., M. Stephens, and J. Pritchard. 2003. Inference of population structure using multilocus genotype data: linked loci and correlated allele frequencies. *Genetics* **164:** 1567–1587.

Figuerola, B., D. K. A. Barnes, P. Brickle, and P. E. Brewin. 2017. Bryozoan diversity around the Falkland and South Georgia Islands: overcoming Antarctic barriers. *Mar. Environ. Res.* **126:** 81–94.

Folmer, O., M. Black, W. Hoeh, R. Lutz, and R. Vrijenhoek. 1994. DNA primers for amplification of mitochondrial cytochrome *c* oxidase subunit I from diverse metazoan invertebrates. *Mol. Mar. Biol. Biotechnol.* **3:** 294–299.

Frichot, E., and O. François. 2015. LEA: an R package for landscape and ecological association studies. *Methods Ecol. Evol.* **6:** 925–929.

Frichot, E., F. Mathieu, T. Trouillon, G. Bouchard, and O. François. 2014. Fast and efficient estimation of individual ancestry coefficients. *Genetics* **196:** 973–983.

Fu, Y. X., and W. H. Li. 1993. Statistical tests of neutrality of mutations. *Genetics* **133:** 693–709.

Galaska, M. P., C. J. Sands, S. R. Santos, A. R. Mahon, and K. M. Halanych. 2017a. Data from: Crossing the divide: admixture across the Antarctic Polar Front revealed by the brittle star *Astrotoma agassizii*. [Online]. Dryad Digital Repository. Available: http://dx.doi.org/10.5061/dryad.3q471 [2017, June 15].

Galaska, M. P., C. J. Sands, S. R. Santos, A. R. Mahon, and K. M. Halanych. 2017b. Geographic structure in the Southern Ocean circumpolar brittle star *Ophionotus victoriae* (Ophiuridae) revealed from mtDNA and single-nucleotide polymorphism data. *Ecol. Evol.* **7:** 1–11.

Goudet, J. 2005. HIERFSTAT, a package for R to compute and test hierarchical *F*-statistics. *Mol. Ecol. Notes* **5:** 184–186.

Heimeier, D., S. Lavery, and M. Sewell. 2010. Molecular species identification of *Astrotoma agassizii* from planktonic embryos: further evidence for a cryptic species complex. *J. Hered.* **101:** 775–779.

Helmuth, B., R. R. Veit, and R. Holberton. 1994. Long-distance dispersal of a subantarctic brooding bivalve (*Gaimardia trapesina*) by kelp-rafting. *Mar. Biol.* **120:** 421–426.

Hempel, G. 1985. *On the Biology of Polar Seas, Particulary the Southern Ocean*, J. S. Gray and M. E. Christiansen, eds. Wiley, Chichester.

Hunter, R. L., and K. M. Halanych. 2008. Evaluating connectivity in the brooding brittle star *Astrotoma agassizii* across the Drake Passage in the Southern Ocean. *J. Hered.* **99:** 137–148.

Jakobsson, M., and N. A. Rosenberg. 2007. CLUMPP: a cluster matching and permutation program for dealing with label switching and multimodality in analysis of population structure. *Bioinformatics* **23:** 1801–1806.

Johnson, G. C., and H. L. Bryden. 1989. On the size of the Antarctic Circumpolar Current. *Deep Sea Res. Part A Oceanogr. Res. Pap.* **36:** 39–53.

Jombart, T. 2008. adegenet: a R package for the multivariate analysis of genetic markers. *Bioinformatics* **24:** 1403–1405.

Jombart, T., and I. Ahmed. 2011. adegenet 1.3-1: new tools for the analysis of genome-wide SNP data. *Bioinformatics* **27:** 3070–3071.

Jombart, T., S. Devillard, and F. Balloux. 2010. Discriminant analysis of principal components: a new method for the analysis of genetically structured populations. *BMC Genet.* **11:** 1–15.

Jörger, K. M., M. Schrödl, E. Schwabe, and L. Würzberg. 2014. A glimpse into the deep of the Antarctic Polar Front—diversity and abundance of abyssal molluscs. *Deep. Sea Res. Part II Top. Stud. Oceanogr.* **108:** 93–100.

Joyce, T. M., S. L. Patterson, and R. C. Millard. 1981. Anatomy of a cyclonic ring in the Drake Passage. *Deep Sea Res. Part A Oceanogr. Res. Pap.* **28:** 1265–1287.

Kaiser, S., S. N. Brandão, S. Brix, D. K. A. Barnes, D. A. Bowden, J. Ingels, F. Leese, S. Schiaparelli, C. P. Arango, R. Badhe, *et al.* 2013. Patterns, processes and vulnerability of Southern Ocean benthos: a decadal leap in knowledge and understanding. *Mar. Biol.* **160:** 2295–2317.

Kalinowski, S. T. 2011. The computer program STRUCTURE does not reliably identify the main genetic clusters within species: simulations and implications for human population structure. *Heredity* **106:** 625–632.

Lamare, M. D., and B. G. Stewart. 1998. Mass spawning by the sea urchin *Evechinus chloroticus* (Echinodermata: Echinoidea) in a New Zealand fiord. *Mar. Biol.* **132:** 135–140.

Leese, F., A. Kop, J.-W. Wägele, and C. Held. 2008. Cryptic speciation in a benthic isopod from Patagonian and Falkland Island waters and the impact of glaciations on its population structure. *Front. Zool.* **5:** 19.

Leese, F., S. Agrawal, and C. Held. 2010. Long-distance island hopping without dispersal stages: transportation across major zoogeographic barriers in a Southern Ocean isopod. *Naturwissenschaften* **97:** 583–594.

Leigh, J. W., and D. Bryant. 2015. POPART: full-feature software for haplotype network construction. *Methods Ecol. Evol.* **6:** 1110–1116.

Librado, P., and J. Rozas. 2009. DnaSP v5: a software for comprehensive analysis of DNA polymorphism data. *Bioinformatics* **25:** 1451–1452.

Meirmans, P. G., and P. H. Van Tienderen. 2004. GENOTYPE and GENODIVE: two programs for the analysis of genetic diversity of asexual organisms. *Mol. Ecol. Notes* **4:** 792–794.

Meredith, M. P., and J. C. King. 2005. Rapid climate change in the ocean west of the Antarctic Peninsula during the second half of the 20th century. *Geophys. Res. Lett.* **32:** 1–5.

Meyer, E. 2017. The Meyer Lab: bioinformatic scripts. [Online]. Oregon State University, Corvallis. Available: https://github.com/Eli-Meyer [2016, Dec. 20].

Nikula, R., C. I. Fraser, H. G. Spencer, and J. M. Waters. 2010. Circumpolar dispersal by rafting in two subantarctic kelp-dwelling crustaceans. *Mar. Ecol. Prog. Ser.* **405:** 221–230.

Palumbi, S. R. 2007. Nucleic acids II: the polymerase chain reaction. Pp. 205–245 in *Molecular Systematics*, 2nd ed., D. M. Hillis, C. Moritz, and B. K. Mable, eds. Sinauer, Sunderland, MA.

Price, J. F., R. A. Weller, and R. R. Schudlich. 1988. Wind-driven ocean currents and Ekman transport. *Deep Sea Res. Part B Oceanogr. Lit. Rev.* **35:** 517.

Pritchard, J. K., M. Stephens, and P. Donnelly. 2000. Inference of population structure using multilocus genotype data. *Genetics* **155:** 945–959.

R Core Team. 2016. R: a language and environment for statistical computing. [Online]. R Foundation for Statistical Computing, Vienna. Available: http://www.R-project.org/ [2017, August 22].

Rasmussen, K., D. M. Palacios, J. Calambokidis, M. T. Saborío, L. Dalla Rosa, E. R. Secchi, G. H. Steiger, J. M. Allen, and G. S. Stone. 2007. Southern Hemisphere humpback whales wintering off

Central America: insights from water temperature into the longest mammalian migration. *Biol. Lett.* **3:** 302–305.

Rosenberg, N. A. 2004. DISTRUCT: a program for the graphical display of population structure. *Mol. Ecol. Notes* **4:** 137–138.

Sands, C. J., T. D. O'Hara, D. K. A. Barnes, and R. Martín-Ledo. 2015. Against the flow: evidence of multiple recent invasions of warmer continental shelf waters by a Southern Ocean brittle star. *Front. Ecol. Evol.* **3:** 1–13.

Smetacek, V., H. J. W. De Baar, U. V. Bathmann, K. Lochte, and M. M. Rutgers Van Der Loeff. 1997. Ecology and biogeochemistry of the Antarctic Circumpolar Current during austral spring: a summary of Southern Ocean JGOFS cruise ANT X/6 of R.V. *Polarstern. Deep. Res. Part II Top. Stud. Oceanogr.* **44:** 1–21.

Stanwell-Smith, D., L. S. Peck, A. Clarke, A. W. A. Murray, and C. D. Todd. 1999. The distribution, abundance and seasonality of pelagic marine invertebrate larvae in the maritime Antarctic. *Philos. Trans. R. Soc. Lond. B Biol. Sci.* **354:** 471–484.

Stöhr, S., T. D. O'Hara, and B. Thuy. 2012. Global diversity of brittle stars (Echinodermata: Ophiuroidea). *PLoS One* **7:** e31940.

Swofford, D. L. 2003. *PAUP*. Phylogenetic Analysis Using Parsimony (*and Other Methods),* Ver. 4. Sinauer, Sunderland, MA.

Tajima, F. 1989. Statistical method for testing the neutral mutation hypothesis by DNA polymorphism. *Genetics* **123:** 585–595.

Tamura, K., G. Stecher, D. Peterson, A. Filipski, and S. Kumar. 2013. MEGA6: molecular evolutionary genetics analysis version 6.0. *Mol. Biol. Evol.* **30:** 2725–2729.

Thatje, S. 2012. Effects of capability for dispersal on the evolution of diversity in Antarctic benthos. *Integr. Comp. Biol.* **52:** 470–482.

Thornhill, D. J., A. R. Mahon, J. L. Norenburg, and K. M. Halanych. 2008. Open-ocean barriers to dispersal: a test case with the Antarctic Polar Front and the ribbon worm *Parborlasia corrugatus* (Nemertea: Lineidae). *Mol. Ecol.* **17:** 5104–5117.

Wang, S., E. Meyer, J. K. McKay, and M. V. Matz. 2012. 2b-RAD: a simple and flexible method for genome-wide genotyping. *Nat. Methods* **9:** 808–810.

Wares, J. P. 2010. Natural distributions of mitochondrial sequence diversity support new null hypotheses. *Evolution* **64:** 1136–1142.

White, W. B., and R. G. Peterson. 1996. An Antarctic circumpolar wave in surface pressure, wind, temperature and sea-ice extent. *Nature* **380:** 699–702.

Wickham, H. 2009. *ggplot2: Elegant Graphics for Data Analysis.* Springer, New York.

Appendix

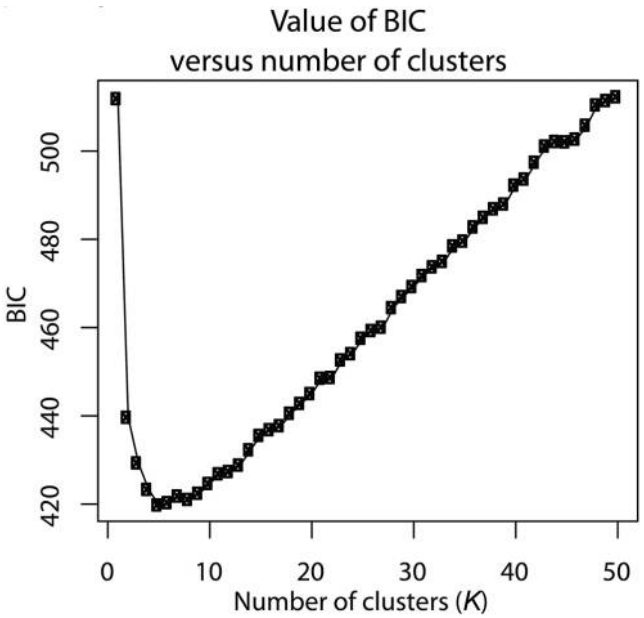

Figure A1. Optimal *K* graph based on Bayesian information criterion (BIC) values for discriminant analyses of principal components.

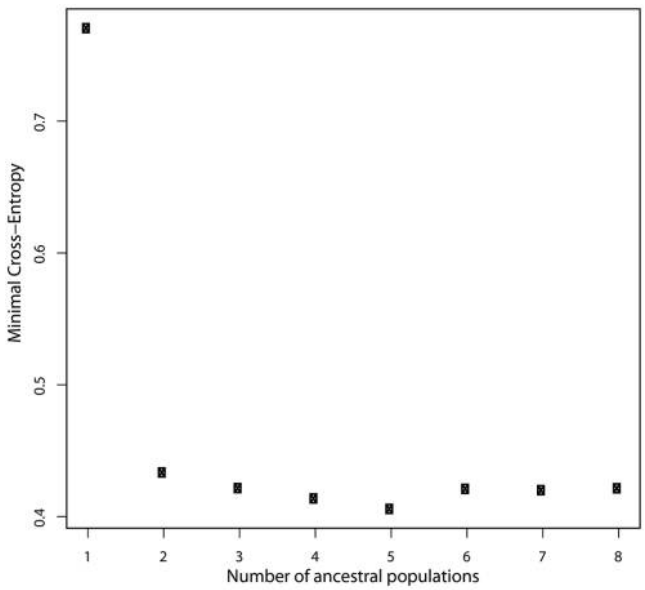

Figure A2. Optimal *K* graph based on minimal cross entropy for admixture analyses in LEA (ver. 1.0; Frichot and François, 2015).

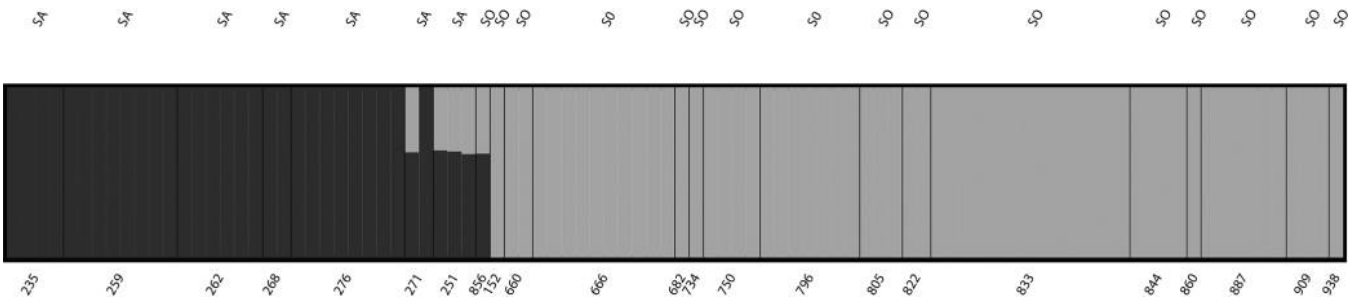

Figure A3. Patterns of population structure for *Astrotoma agassizii* in both the Southern Ocean (SO) and South America (SA) based on single-nucleotide polymorphism data analyzed in STRUCTURE (ver. 2.3.4; Falush *et al.*, 2003) and visualized in DISTRUCT (Rosenberg, 2004), testing for the true number of populations (*K*). $K = 2$ is presented in the graph as our most likely value of *K*.

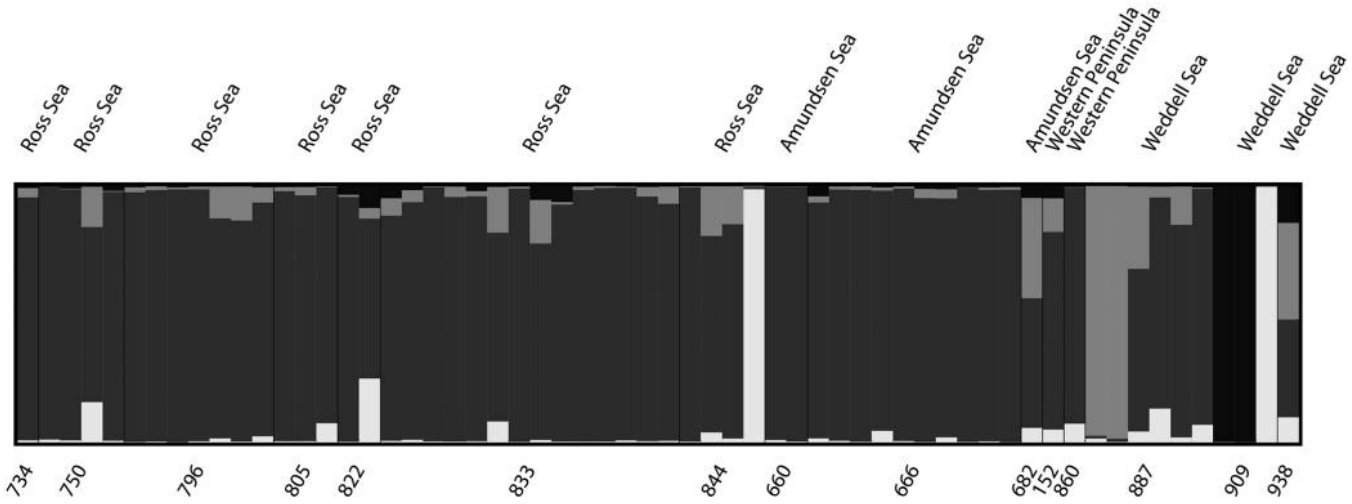

Figure A4. Patterns of population structure for *Astrotoma agassizii* in the Southern Ocean based on single-nucleotide polymorphism data analyzed in STRUCTURE (ver. 2.3.4; Falush *et al.*, 2003) and visualized in DISTRUCT (Rosenberg, 2004), testing for the true number of populations (K). $K = 4$ is presented in the graph as our most likely value of K.

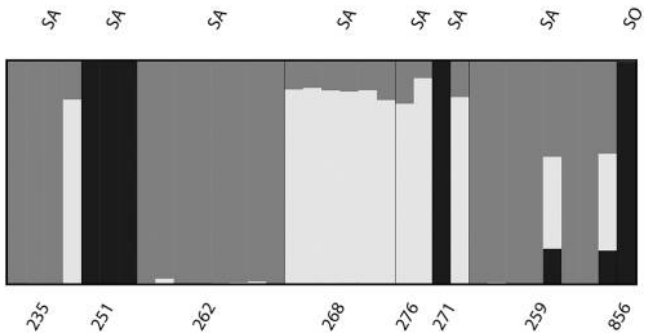

Figure A5. Patterns of population structure for *Astrotoma agassizii* in South American (SA) waters and Op856_2e from the Southern Ocean (SO) based on single-nucleotide polymorphism data analyzed in STRUCTURE (ver. 2.3.4; Falush *et al.*, 2003) and visualized in DISTRUCT (Rosenberg, 2004), testing for the true number of populations (K). $K = 3$ is presented in the graph as our most likely value of K.

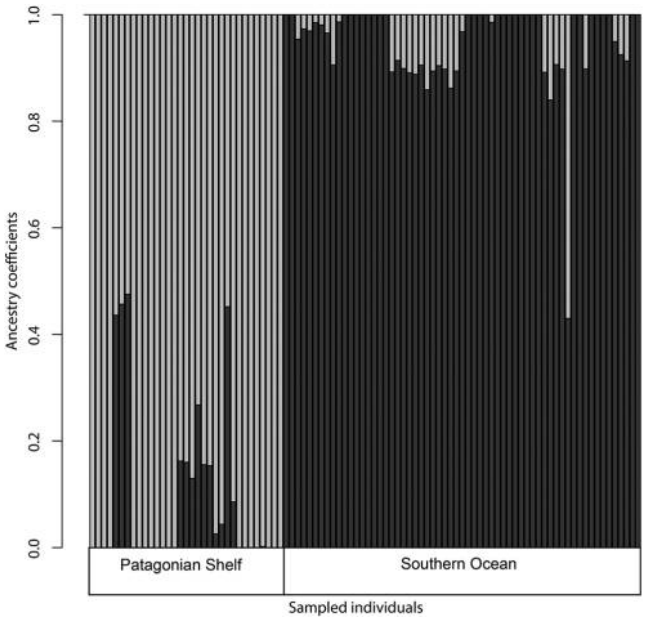

Figure A6. Admixture of *Astrotoma agassizii* from the South American Patagonian Shelf and from the Southern Ocean analyzed in LEA (ver. 1.0; Frichot and François, 2015), assuming $K = 2$.